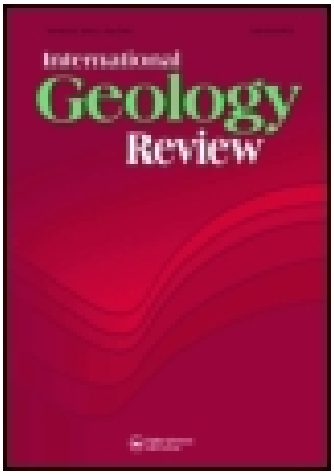

International Geology Review
Publication details, including instructions for authors and subscription information:
http://www.tandfonline.com/loi/tigr20

U-Pb zircon ages, geochemical and Sr-Nd-Pb isotopic constraints on the dating and origin of intrusive complexes in the Sulu orogen, eastern China

Shen Liu [a b], Ruizhong Hu [a], Shan Gao [b], Caixia Feng [b], Hong Zhong [a], Youqiang Qi [b], Tao Wang [b], Guangying Feng [b] & Yuhong Yang [c]

[a] State Key Laboratory of Ore Deposit Geochemistry, Institute of Geochemistry, Chinese Academy of Sciences, Guiyang, 550002, China

[b] State Key Laboratory of Geological Processes and Mineral Resources, China University of Geosciences, Wuhan, 430074, China

[c] Solid Earth Studies Laboratory, Department of Geology, University of Regina, Regina, Saskatchewan, S4S 0A2, Canada

Published online: 27 Apr 2009.

To cite this article: Shen Liu, Ruizhong Hu, Shan Gao, Caixia Feng, Hong Zhong, Youqiang Qi, Tao Wang, Guangying Feng & Yuhong Yang (2011) U-Pb zircon ages, geochemical and Sr-Nd-Pb isotopic constraints on the dating and origin of intrusive complexes in the Sulu orogen, eastern China, International Geology Review, 53:1, 61-83, DOI: 10.1080/00206810902900319

To link to this article: http://dx.doi.org/10.1080/00206810902900319

International Geology Review
Vol. 53, No. 1, 10 January 2011, 61–83

Taylor & Francis
Taylor & Francis Group

U–Pb zircon ages, geochemical and Sr–Nd–Pb isotopic constraints on the dating and origin of intrusive complexes in the Sulu orogen, eastern China

Shen Liu[ab]*, Ruizhong Hu[a], Shan Gao[b], Caixia Feng[b], Hong Zhong[a], Youqiang Qi[b], Tao Wang[b], Guangying Feng[b] and Yuhong Yang[c]

[a]*State Key Laboratory of Ore Deposit Geochemistry, Institute of Geochemistry, Chinese Academy of Sciences, Guiyang 550002, China;* [b]*State Key Laboratory of Geological Processes and Mineral Resources, China University of Geosciences, Wuhan 430074, China;* [c]*Solid Earth Studies Laboratory, Department of Geology, University of Regina, Regina, Saskatchewan S4S 0A2, Canada*

(*Accepted 16 March 2009*)

TPost-orogenic intrusive complexes from the Sulu belt of eastern China consist of pyroxene monzonites and dioritic porphyrites. We report new U–Pb zircon ages, geochemical data, and Sr–Nd–Pb isotopic data for these rocks. Laser ablation-inductively coupled plasma-mass spectrometry U–Pb zircon analyses yielded a weighted mean $^{206}Pb/^{238}U$ age of 127.4 ± 1.2 Ma for dioritic porphyrites, consistent with crystallization ages (126 Ma) of the associated pyroxene monzonites. The intrusive complexes are characterized by enrichment in light rare earth elements and large ion lithophile elements (i.e. Rb, Ba, Pb, and Th) and depletion in heavy rare earth elements and high field strength elements (i.e. Nb, Ta, P, and Ti), high $(^{87}Sr/^{86}Sr)_i$ ranging from 0.7083 to 0.7093, low $\varepsilon_{Nd}(t)$ values from ε14.6 to − 19.2, $^{206}Pb/^{204}Pb$ = 16.65–17.18, $^{207}Pb/^{204}Pb$ = 15.33–15.54, and $^{208}Pb/^{204}Pb$ = 36.83–38.29. Results suggest that these intermediate plutons were derived from different sources. The primary magma-derived pyroxene monzonites resulted from partial melting of enriched mantle hybridized by melts of foundered lower crustal eclogitic materials before magma generation. In contrast, the parental magma of the dioritic porphyrites was derived from partial melting of mafic lower crust beneath the Wulian region induced by the underplating of basaltic magmas. The intrusive complexes may have been generated by subsequent fractionation of clinopyroxene, potassium feldspar, plagioclase, biotite, hornblende, ilmenite, and rutile. Neither was affected by crustal contamination. Combined with previous studies, these findings provide evidence that a Neoproterozoic batholith lies beneath the Wulian region.

Keywords: intrusive complexes; foundering; underplating; Sulu belt; eastern China

Introduction

The Sulu orogenic belt is generally accepted as the eastern part of the Qinling–Dabie collisional orogenic belt sited between the north China and Yangtze blocks (e.g. Yin and Ni 1993; Xu and Zhu 1994; Cong 1996; Jahn *et al.* 1996; Ye *et al.* 1996, 2000; Li *et al.* 1999; Zheng *et al.* 2002). High pressure to ultrahigh pressure (HP–UHP) metamorphic rocks, such as those found at Rizhao, Qingdao, and Weihai (Cong 1996; Jahn *et al.* 1996; Ye *et al.* 1996; Zheng *et al.* 2003), Neoproterozoic magmatic rocks, such as granites and

*Corresponding author. Email: liushen@vip.gyig.ac.cn

ISSN 0020-6814 print/ISSN 1938-2839 online

DOI: 10.1080/00206810902900319
http://www.informaworld.com

gabbros (Zhou *et al.* 2003b; Wu *et al.* 2004; Huang *et al.* 2005), and voluminous syn-collisional and post-collisional magmatic rocks, such as alkaline complexes (Chen *et al.* 2003; Guo *et al.* 2005; Yang *et al.* 2005a,b), volcanic rocks (Fan *et al.* 2001; Guo *et al.* 2004), granitoids and diorites (Zhao *et al.* 1997; Zhou and Lu 2000; Hong *et al.* 2003; Huang *et al.* 2005; Yang *et al.* 2005a,b), gabbros (Meng *et al.* 2005), volcanic-intrusive complexes (BGMRS 1991a; Zhou *et al.* 2003a), mafic dikes (Guo *et al.* 2004; Yang *et al.* 2005a,b; Liu *et al.* 2008a,b), and adakites (Guo *et al.* 2006; Liu *et al.* 2009) are widespread and mark the zone of collision. These rocks contain valuable information on deep dynamic processes, and can be used to study the orogenic processes of continental subduction and the role of crust–mantle interaction (Menzies and Kyle 1990; Jahn *et al.* 1996; Ye *et al.* 2000; Fan *et al.* 2001; Guo *et al.* 2004).

The Mesozoic magamatic rocks widely distributed in the Sulu orogenic belt mainly formed between 225 and 114 Ma (Zhao *et al.* 1997; Zhou and Lu 2000; Fan *et al.* 2001; Chen *et al.* 2003; Zhou *et al.* 2003a; Guo *et al.* 2004, 2005, 2006; Huang *et al.* 2005; Meng *et al.* 2005; Yang *et al.* 2005a,b); they consist dominantly of intermediate-acid igneous rocks. In contrast, the distributions of these Mesozoic mafic rocks are limited, and most of them are distributed in the form of dikes (BGMRS 1991b; Cheng *et al.* 1998; Yang and Zhou 2001; Guo *et al.* 2004) as only small-scale basalt extrusions and mafic intrusions (Fan *et al.* 2001; Meng *et al.* 2005). These widespread Mesozoic intermediate-acid rocks are considered to be the result of recycling of the subducted Yangtze cratonic continental crust (Zheng *et al.* 2003; Zhao *et al.* 2004, 2005; Yang *et al.* 2005a,b). However, the Pb isotopic compositions of the majority of intermediate-acid rocks in the Sulu orogenic belt are significantly different to those of the Yangtze lithospheric mantle, and are similar to those of the mafic rocks from the central north China craton (Xie *et al.* 2006; Liu *et al.* 2008a,b). Moreover, the origins of the adakitic volcanic rocks from the Sulu orogenic belt argue against the contribution of the Yangtze lithosphere (Guo *et al.* 2006; Liu *et al.* 2009). As such, the generation of the intermediate-acid rocks in the Sulu orogenic belt may not be due to the involvement of the subducted Yangtze continental crust. Consequently, it is important to undertake further investigations into the Mesozoic intermediate-acid rocks in the Sulu orogentic belt.

The Qibaoshan intrusive complex, which is exposed in the Wulian region in the northwest part of the Sulu orogenic belt and is comprised of an intrusive association of pyroxene monzonite–dioritic porphyrite (Figure 1), is one such example. In this paper, we present petrographic, geochronological, geochemical, and Sr–Nd–Pb isotopic data on these rocks. These data are used to discuss their petrogenesis. Interpretation of the data then leads to an integrated model of intrusive complexes in a post-orogenic setting.

Geological setting and petrography

Voluminous Neoproterozoic and Mesozoic magmatic rocks outcrop in the Wulian region, northwest of the Sulu terrane (Zhou *et al.* 2003b; Wu *et al.* 2004; Huang *et al.* 2005). The Neoproterozoic rocks have widely undergone greenschist facies metamorphism, and they contain gneissic granites, plagioamphibolites and quartzite–carbonaceous slate-phyllite-marble associations; in contrast, granite is the dominant Mesozoic rock type in the Wulian region (Huang *et al.* 2005). The studied region is located in a triangular area created by the connection of three faults. The granites and diorites are the dominant rock types, making up more than 98% of the Meosozoic magmatic rocks in the Wulian region. The Qibaoshan complex is influenced by the Tanlu Fault to the west, the Wulian-Weihai Fault to the east, and the Beixing–Xuejiaguanzhuang–Huigouzi–Dingjiaguanzhuang Fault to the north.

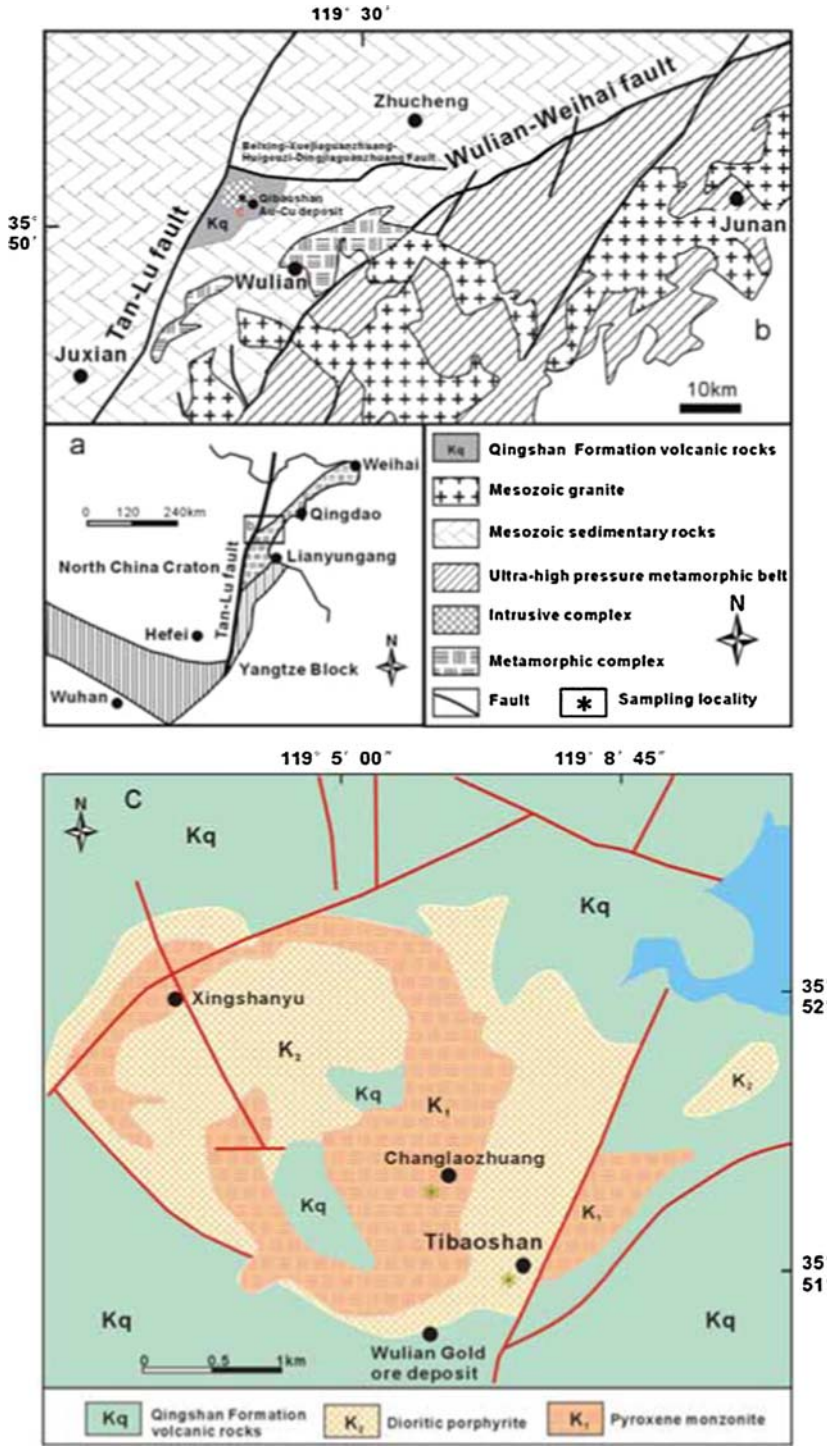

Figure 1. (a) Simplified tectonic map of the Sulu belt, eastern China (modified after Guo *et al.* 2004). (b,c) A geologic map of the study areas and the distribution of the intrusive complexes (modified after BGMRS 1991b).

The Qibaoshan complex is exposed for ca. 12 km^2, and is bounded by Qingshan Formation volcanic rocks (Figure 1(b)). The zircon U–Pb age for pyroxene monzonite is 126 ± 3 Ma (Zhou *et al.* 2003a,b), and this age is used in this paper for the age-correction of the Nd, Sr, and Pb isotopic compositions.

The pyroxene monzonites are grey-black, fine- to medium-grained, with a massive texture. They are composed of subhedral clinopyroxene (10%; 1.2 mm), orthopyroxene (10%; 1.0 mm), plagioclase (40%; 1.0–1.2 mm), biotite (5%; 1.0–1.2 mm), and orthoclase (35%; 1.2–1.5 mm). Accessory minerals include apatite, zircon, magnetite, and titanite.

The dioritic porphyrites are light grey, fine- to medium-grained with massive and porphyritic textures. The rocks contain 30% phenocrysts, which consist of plagioclase (An = 30–50; 80–85%; 1.0–2.0 mm), hornblende (8–10%; 1.0–2.0 mm), biotite (2–5%; 1.0 mm), and K-feldspar (5%; 1.0–1.2 mm). 70% of the matrix is composed of plagioclase and cryptocrystalline. Accessory minerals include zircon, apatite, titanite, magnetite, and ilmenite.

Analytical methods

Laser ablation techniques were used in zircon age determination (Table 1). The analyses were conducted with an Elan 6100 DRC ICP-MS equipped with 193 nm Excimer lasers, which is housed in the Department of Geology, Northwest University, Xi'an, China. Zircon 91500 was used as a standard, with a spot size of 30 μm. Raw data was reduced using the GLITTER program. The detailed analytical procedures are described by Yuan *et al.* (2004).

Whole-rock samples were trimmed to remove the altered surfaces, and were cleaned with deionized water, crushed, and powdered with an agate mill. The pulverized samples were used for major element, trace element, and Sr–Nd–Pb isotopic analyses.

The major elements were analysed with a PANalytical Axios-advance (Axios PW4400) X-ray fluorescence spectrometer (XRF) at the State Key Laboratory of Ore Deposit Geochemistry, Institute of Geochemistry, Chinese Academy of Sciences (IGCAS). Fused glass disks were used and the analytical precision, as determined on the Chinese National standards GSR-1 and GSR-3, was better than 5% (Table 2). Loss on ignition (LOI) was obtained using 1 g powder heated to 1100°C for 1 h. Trace elements were analysed with a POEMS ICP-MS at the National Research Centre of Geoanalysis, the Chinese Academy of Geosciences, following the procedures described by Qi *et al.* (2000). The discrepancy between the triplicates is less than 5% for all of the elements. The analyses with the international standards OU-6 and GBPG-1 are in agreement with the recommended values (Table 2).

For the Rb–Sr and Sm–Nd isotope analyses, sample powders were spiked with mixed isotope tracers, dissolved in Teflon capsules with HF + HNO_3 acid, and separated by the conventional cation-exchange technique. Isotopic measurements were performed on a Finnigan MAT-262 thermal ionization mass spectrometer at the Isotopic Geochemistry Laboratory of the Yichang Institute of Geology and Mineral Resources. Procedural blanks were $<$200 pg for Sm and Nd, and $<$500 pg for Rb and Sr. The mass fractionation corrections for the Sr and Nd isotopic rations were based on $^{86}Sr/^{88}Sr = 0.1194$ and $^{146}Nd/^{144}Nd = 0.7219$, respectively. The analyses of the standards used during the period of analysis are as follows: NBS987 gave $^{87}Sr/^{86}Sr = 0.710246 \pm 16(2\sigma)$; La Jolla gave $^{143}Nd/^{144}Nd = 0.511863 \pm 8$ (2σ). Pb was separated and purified by the conventional cation-exchange technique (AG1 × 8, 200–400 resin) with diluted HBr as the eluant. Analyses of NBS981 during the period of analysis yielded $^{204}Pb/^{206}Pb = 0.0896 \pm 15$, $^{207}Pb/^{206}Pb = 0.9145 \pm 8$, and $^{208}Pb/^{206}Pb = 2.162 \pm 2$ (Table 3).

Table 1. Laser ablation ICP-MS U–Pb data of zircons in the dioritic porphyrites (QBS001) from Wulian region, Sulu orogenic belt, eastern NCC.

	Isotopic ratios						Age (Ma)					
Spot $^{238}U/^{232}Th$	$^{207}Pb/^{206}Pb$	1σ	$^{207}Pb/^{235}U$	1σ	$^{206}Pb/^{238}U$	1σ	$^{207}Pb/^{206}Pb$	1σ	$^{207}Pb/^{235}U$	1σ	$^{206}Pb/^{238}U$	1σ
0.68	0.05634	0.0017	0.15815	0.0045	0.02036	0.0002	466	47	149	4	130	1
0.81	0.05189	0.0033	0.14122	0.0087	0.01974	0.0003	281	113	134	8	126	2
1.17	0.06368	0.0009	1.09396	0.0120	0.12461	0.0008	731	13	750	6	757	5
0.51	0.05995	0.0020	0.17015	0.0055	0.02059	0.0002	602	53	160	5	131	1
0.91	0.06479	0.0007	1.11251	0.0086	0.12455	0.0007	768	8	759	4	757	4
0.57	0.10784	0.0028	0.13037	0.0075	0.02088	0.0002	359	191	137	11	124	1
1.49	0.06432	0.0010	1.10979	0.0149	0.12514	0.0009	752	17	758	7	760	5
0.53	0.05127	0.0014	0.14008	0.0035	0.01982	0.0002	253	43	133	3	127	1
2.25	0.04785	0.0008	0.12796	0.0018	0.0194	0.0001	92	22	122	2	124	1
0.78	0.04662	0.0018	0.1326	0.0050	0.02063	0.0002	50	62	126	4	132	1
0.46	0.05316	0.0021	0.14387	0.0053	0.01963	0.0002	336	65	136	5	125	1
0.58	0.04798	0.0018	0.12768	0.0045	0.0193	0.0002	98	64	122	4	123	1
3.10	0.0639	0.0010	1.10157	0.0137	0.12505	0.0008	738	15	754	7	760	5
0.60	0.07167	0.0026	0.18647	0.0064	0.01887	0.0002	417	172	133	9	118	1
1.35	0.06548	0.0011	1.12314	0.0157	0.12441	0.0009	790	18	764	7	756	5
0.73	0.04736	0.0009	0.13157	0.0023	0.02015	0.0001	67	28	126	2	129	1
0.59	0.05396	0.0019	0.14368	0.0048	0.01931	0.0002	369	58	136	4	123	1
0.49	0.04992	0.0022	0.14439	0.0054	0.02069	0.0002	209	16	310	4	132	1
1.72	0.0642	0.0011	1.10629	0.0167	0.12498	0.0009	748	20	756	8	759	5
0.56	0.06155	0.0032	0.16494	0.0084	0.01944	0.0003	96	199	121	10	122	2
1.07	0.06525	0.0008	1.11167	0.0108	0.12358	0.0008	782	11	759	5	751	4
1.70	0.04905	0.0010	0.13956	0.0025	0.02064	0.0001	150	29	133	2	132	1
0.79	0.065	0.0009	1.11063	0.0127	0.12393	0.0008	774	14	758	6	753	5
1.11	0.06624	0.0009	1.14241	0.0121	0.1251	0.0008	814	12	774	6	760	5
0.56	0.05053	0.0022	0.14456	0.0061	0.02075	0.0002	219	78	137	5	132	1
0.53	0.05247	0.0025	0.15401	0.0069	0.02129	0.0003	306	81	145	6	136	2

Table 2. Major oxides (wt.%) and trace elements (ppm) for the intrusive complexes from Wulian region, Sulu orogenic belt, eastern China.

Sample	QBS25	QBS23	QBS22	QBS21	QBS18	QBS15	QBS13	QBS11	QBS10	QBS9	QBS6	QBS5	QBS1	GSR-3	GSR-3	GSR-1	GSR-1
Sample rock type	Dioritic prophyrite					Pyroxene-monzonite								RV*	MV*	RV*	MV*
SiO_2	61.01	61.57	60.86	60.36	59.77	60.91	56.11	55.57	56.29	55.34	55.87	55.71	55.28	44.64	44.75	72.83	72.65
TiO_2	0.64	0.62	0.61	0.61	0.60	0.65	1.02	1.02	1.02	1.02	1.01	1.01	1.01	2.37	2.36	0.29	0.29
Al_2O_3	15.41	15.53	14.66	14.72	14.8	15.39	18.74	18.44	18.65	18.47	18.5	18.63	18.34	13.83	14.14	13.40	13.52
Fe_2O_3	7.29	6.72	9.43	9.16	9.43	7.35	8.08	7.78	7.33	7.58	7.42	7.99	7.85	13.4	13.35	2.14	2.18
MnO	0.35	0.42	0.38	0.35	0.58	0.30	0.14	0.07	0.13	0.06	0.07	0.08	0.07	0.17	0.16	0.06	0.06
MgO	3.98	3.81	3.44	2.97	2.88	4.21	3.38	3.43	3.45	3.54	3.32	3.28	3.29	7.77	7.74	0.42	0.46
CaO	1.26	1.08	0.45	0.47	0.45	1.84	2.30	3.12	1.99	2.58	2.90	2.92	2.89	8.81	8.82	1.55	1.56
Na_2O	0.48	0.38	0.31	0.34	0.30	1.25	3.54	3.24	3.64	3.40	3.21	3.11	3.24	3.38	3.18	3.13	3.15
K_2O	6.97	7.29	6.73	7.13	7.22	6.13	3.65	4.05	3.66	3.75	4.29	4.75	3.60	2.32	2.3	5.01	5.03
P_2O_5	0.29	0.29	0.28	0.28	0.28	0.29	0.77	0.78	0.78	0.77	0.75	0.76	0.75	0.95	0.97	0.09	0.11
LOI	2.15	1.96	2.38	2.97	3.46	1.81	2.12	2.46	2.87	3.25	2.55	1.62	2.98	2.24	2.12	0.70	0.69
Total	99.83	99.66	99.54	99.36	99.77	100.13	99.84	99.95	99.81	99.76	99.88	99.84	99.31	99.88	99.89	99.62	99.7
T_{Zr}(°C)	823	823	812	820	820	815	897	893	914	911	949	948	916	OU-6	OU-6	GBPG-1	GBPG-1
Sc	14.3	14.1	13.3	13.8	13.5	14.5	16.5	16.7	16.9	16.6	16.3	15.8	16.4	22.1	22.4	13.9	13.9
V	110	111	97.7	109	107	114	151	155	153	157	151	154	151	129	131	96.5	103
Cr	92.3	92.0	1141	88.9	79.9	90.1	34.0	35.3	40.3	35.6	39.4	41.5	37.3	70.8	73.5	181	187
Co	19.7	21.3	19.4	19.8	17.0	17.0	16.5	18.3	21.0	19.2	17.6	20.1	17.0	29.1	30.3	19.5	20.2
Ni	49.3	47.1	41.0	43.9	40.7	47.0	25.4	29.2	26.7	35.1	27.0	28.9	27.4	39.8	40.5	59.6	60.6
Ga	19.8	19.3	17.0	18.6	18.7	18.9	26.8	27.1	26.8	26.7	27.1	26.7	26.9	24.3	24.5	18.6	18.9
Rb	191	194	175	206	210	165	114	122	107	113	122	146	107	120	122	56.2	58.4
Sr	242	244	168	217	189	253	1085	1292	1070	1158	1257	1277	1112	131	136	364	367
Y	14.1	15.7	13.8	14.7	14.3	14.3	28.1	28.5	28.3	28.4	29.1	29.1	27.8	27.4	26.8	18.0	17.5
Zr	131	129	107	120	121	131	305	323	352	361	526	530	384	174	173	232	234
Nb	9.81	9.84	8.41	9.62	9.31	9.82	34.2	32.4	31.8	32.4	35.8	33.9	33.1	14.8	15.1	9.93	9.74
Ba	4816	4637	3245	4224	3831	3925	2664	3181	2693	2954	3307	3326	2872	477	482	908	913
La	58.9	58.3	56.4	59.8	53.8	51.7	211	211	207	213	211	212	206	33.0	33	53.0	51
Ce	113	112	104	112	102	103	403	402	394	406	401	405	391	74.4	76	103	105
Pr	11.7	11.8	10.7	11.7	10.9	11.0	39.3	39.2	38.7	39.6	39.3	39.6	38.7	7.80	8.1	11.5	11.6
Nd	43.0	42.8	37.4	41.8	39.6	40.6	132	133	129	135	132	133	129	29.0	30.6	43.3	42.4
Sm	6.74	6.76	5.55	6.10	6.06	6.58	17.3	17.8	17.0	17.6	17.3	17.3	17.0	5.92	5.99	6.79	6.63

Table 2 – *continued*

Sample rock type	QBS25	QBS23	QBS22	QBS21	QBS18	QBS15	QBS13	QBS11	QBS10	QBS9	QBS6	QBS5	QBS1	GSR-3 RV*	GSR-3 MV*	GSR-1 RV*	GSR-1 MV*
	Dioritic prophyrite					Pyroxene-monzonite											
Eu	1.71	1.52	1.03	1.16	1.28	1.57	3.09	3.19	2.99	3.10	3.07	3.08	3.12	1.36	1.35	1.79	1.69
Gd	5.59	5.31	4.23	4.55	4.50	5.50	11.1	11.0	10.5	11.2	11.0	11.1	11.0	5.27	5.50	4.74	4.57
Tb	0.60	0.64	0.53	0.57	0.56	0.59	1.31	1.30	1.25	1.29	1.31	1.32	1.26	0.85	0.83	0.60	0.59
Dy	2.93	3.26	2.75	3.03	2.92	3.00	5.97	6.09	5.90	6.10	6.12	6.15	5.97	4.99	5.06	3.26	3.17
Ho	0.56	0.59	0.51	0.58	0.56	0.55	1.08	1.07	1.03	1.09	1.07	1.09	1.06	1.01	1.02	0.69	0.66
Er	1.57	1.59	1.51	1.67	1.65	1.55	3.19	3.18	3.14	3.16	3.19	3.24	3.11	2.98	3.07	2.01	2.02
Tm	0.21	0.23	0.19	0.22	0.21	0.21	0.40	0.40	0.40	0.41	0.40	0.41	0.40	0.44	0.45	0.30	0.29
Yb	1.37	1.40	1.28	1.42	1.35	1.34	2.67	2.60	2.69	2.65	2.70	2.71	2.70	3.00	3.09	2.03	2.03
Lu	0.21	0.21	0.19	0.22	0.21	0.21	0.39	0.39	0.40	0.40	0.42	0.40	0.39	0.45	0.47	0.31	0.31
Hf	3.45	3.32	2.88	3.28	3.30	3.47	6.55	6.81	7.38	7.67	10.3	10.6	8.15	4.70	4.86	6.07	5.96
Ta	0.52	0.57	0.45	0.52	0.51	0.54	1.30	1.24	1.27	1.24	1.38	1.32	1.32	1.06	1.03	0.40	0.42
Pb	5635	7188	856	898	953	1716	53.6	32.5	46.7	34.2	28.3	32.2	33.8	28.2	32.7	14.1	14.5
Th	14.1	14.6	11.9	14.2	13.6	14.3	85.7	82.9	83.7	86.0	91.9	89.2	88.1	11.5	11.9	11.2	11.4
U	2.73	5.06	7.33	6.11	8.99	2.59	10.1	10.5	9.20	9.34	11.5	11.4	10.0	1.96	2.09	0.90	0.92
$(La/Yb)_N$	30.8	30.0	31.7	30.2	28.6	27.8	56.7	58.3	55.1	57.6	55.9	56.1	54.7				
Eu/Eu^*	0.85	0.77	0.65	0.67	0.75	0.80	0.68	0.70	0.69	0.67	0.68	0.68	0.70				

Note: LOI, loss on ignition; RV*, recommended values; MV*, measured values. The values for GSR-1 and GSR-3 from Wang *et al.* (2003), for GBPG-1 from Thompson *et al.* (2000) and for OU-6 from Potts and Kane (2005).

Table 3. Sr–Nd–Pb isotopic compositions for the intrusive complexes from Wulian, Sulu orogenic belt, eastern China.

Sample no.	Age (Ma)	$^{147}Sm/^{144}Nd$	$^{143}Nd/^{144}Nd$	2σ	$(^{143}Nd/^{144}Nd)_i$	$\varepsilon_{Nd}(t)$	$^{87}Rb/^{86}Sr$	$^{87}Sr/^{86}Sr$	2σ	$(^{87}Sr/^{86}Sr)_i$	$^{206}Pb/^{204}Pb$	$^{207}Pb/^{204}Pb$	$^{208}Pb/^{204}Pb$	$(^{206}Pb/^{204}Pb)_i$	$(^{207}Pb/^{204}Pb)_i$	$(^{208}Pb/^{204}Pb)_i$
QBS-25	127	0.095	0.51178	10	0.511499	19.0	2.290	0.712395	9	0.708262	17.021	15.407	37.889	17.020	15.407	37.888
QBS-23		0.095	0.511571	11	0.511492	−19.2	2.303	0.712419	13	0.708263	17.096	15.44	37.552	17.095	15.440	37.551
QBS-18		0.092	0.511566	13	0.511489	−19.2	3.215	0.714066	11	0.708264	17.194	15.538	38.296	17.182	15.537	38.290
QBS-15		0.098	0.511575	9	0.511494	−19.1	1.878	0.711656	10	0.708267	17.158	15.469	37.64	17.156	15.469	37.637
QBS-13	126	0.079	0.511787	9	0.511722	−14.7	0.304	0.709847	10	0.709302	16.949	15.338	37.711	16.719	15.327	37.072
QBS-9		0.079	0.511791	10	0.511726	−14.6	0.283	0.709813	11	0.709303	16.986	15.363	37.721	16.652	15.347	36.714
QBS-5		0.079	0.511783	8	0.511718	−14.8	0.331	0.709894	12	0.709302	17.35	15.417	38.009	16.914	15.396	36.890
QBS-1		0.079	0.511793	8	0.511728	−14.6	0.278	0.709801	11	0.709303	17.191	15.369	37.871	16.838	15.352	36.831

Note: Chondrite uniform reservoir values ($^{87}Rb/^{86}Sr = 0.0847$, $^{87}Sr/^{86}Sr = 0.7045$, $^{147}Sm/^{144}Nd = 0.1967$, and $^{143}Nd/^{144}Nd = 0.512638$) are used for the calculation. $\lambda_{Rb} = 1.42 \times 10^{-11}$ year^{-1} (Steiger and Jäer 1977); $\lambda_{Sm} = 6.54 \times 10^{-12}$ year^{-1} (Lugmair and Harti 1978). Corrected-age (126 Ma) for pyroxene monzonites is from Zhou *et al.* (2003a).

Analytical results

Zircon CL images and U–Pb data

Zircons are abundant in dioritic porphyrites. The zircons from dioritic sample QBS001 are euhedral and range up to 100 μm in size, and most of them are transparent and light brown in colour with an oscillatory zoning structure (Figure 2). The zircon U–Pb data are presented in Table 1. Analyses of zircon grains with an oscillatory structure are concordant and yield the two weighted mean $^{206}Pb/^{238}U$ ages of 127.4 ± 1.2 Ma ($n = 17$) and 757 ± 4.8 Ma ($n = 9$; Figure 3). The younger age is interpreted as the crystallization age of the dioritic porphyrites, and the later age as the inherited zircon age.

Major and trace elements

The geochemical data for the pyroxene monzonites and dioritic porphyrites from Qibaoshan are shown in Table 2, and the major oxide contents are illustrated in Figures 4 and 5. In the present study, the pyroxene monzonites are of a higher chemical composition than the dioritic porphyrites, with the exception of certain elements, such as $SiO_2 = 55.28–56.29$ wt%, $K_2O = 3.65–4.75$ wt%, MnO = 0.07–0.14 wt%, Cr = 35.3–41.5 ppm, Ni = 26.7–35.1 ppm, Rb = 107–146 ppm, Ba = 2664–3326 ppm, and Pb = 28.3–53.6 ppm. The pyroxene monzonites and dioritic porphyrites are relatively high in total alkalis, with a value of $K_2O = 3.65–7.29$ wt% and $Na_2O = 0.3–3.64$ wt%, and the total $K_2O + Na_2O$ ranging from 7.05 wt% to 8.18 wt%. On the total alkali–silica (TAS) diagram, all the pyroxene monzonites plot in the alkaline field, whereas the dioritic porphyrites fall into the subalkaline series (Figure 4(a)). In addition, all samples straddle the shoshonitic series in

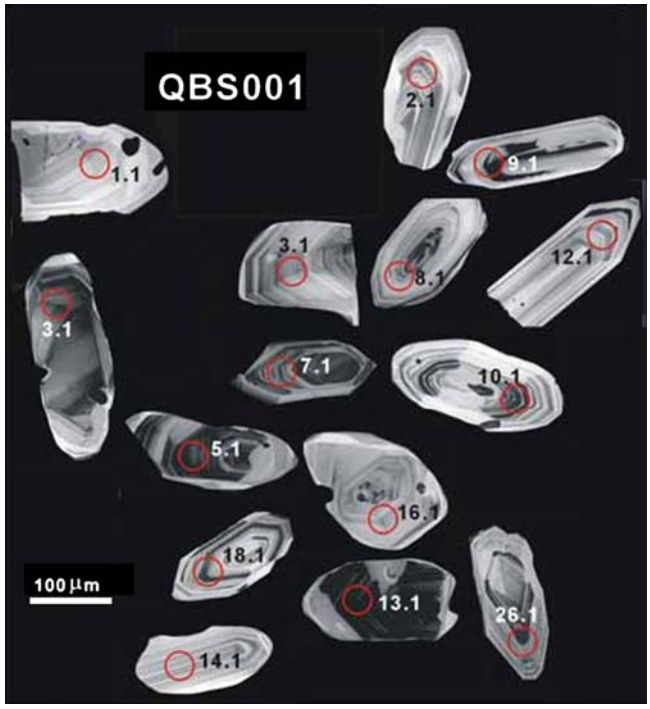

Figure 2. Representative cathodoluminescence images of zircon grains from the dioritic porphyrites (QBS001). The numbers correspond to the spot analyses given in Table 1.

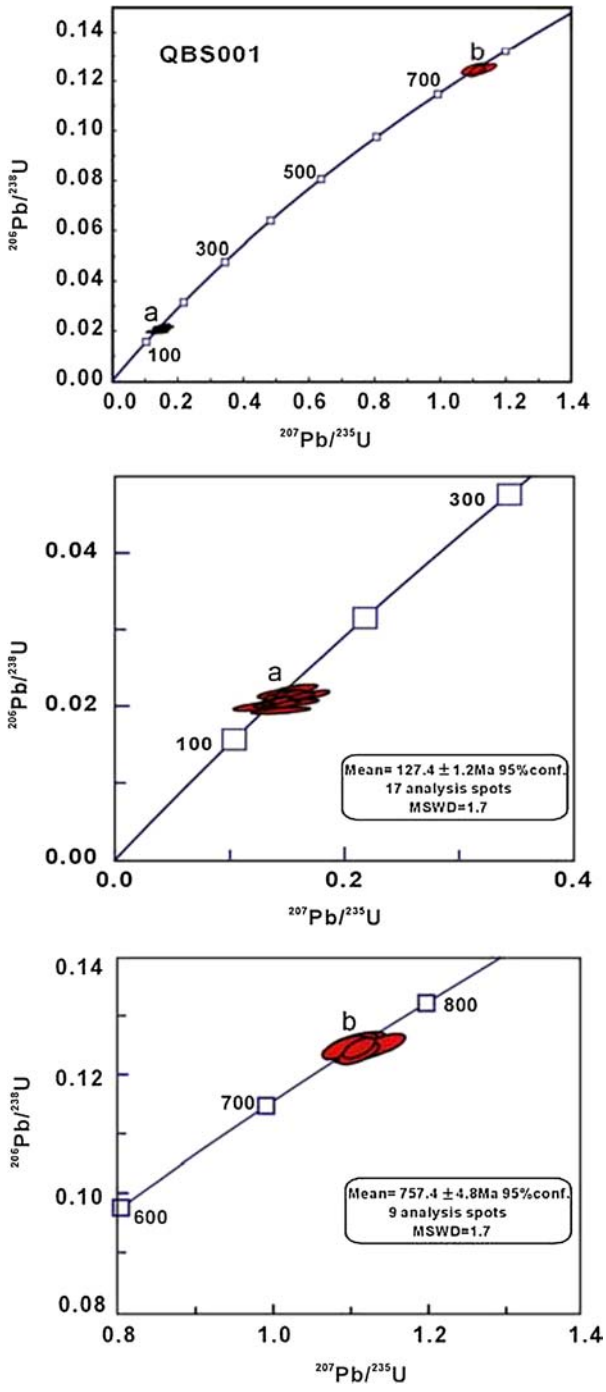

Figure 3. Laser ablation-inductively coupled plasma-mass spectrometry zircon U–Pb concordia diagrams for sample QBS001 from the dioritic porphyrites in the Wulian region, the Sulu belt.

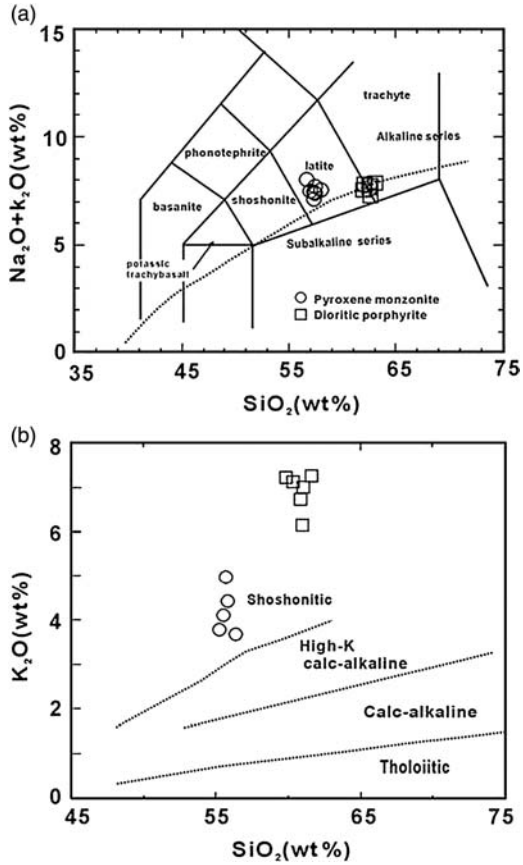

Figure 4. Classification of the pyroxene monzonites and dioritic porphyrites from the Sulu belt on the basis of (a) the TAS diagram. All the major element data have been recalculated to 100% on a LOI-free basis (after Middlemost 1994; Le Maitre 2002); (b) K_2O versus Na_2O diagram, showing the intrusive complexes to be shoshonitic (after Middlemost 1972). The legends in the other figures are the same as in Figure 4.

the Na_2O versus K_2O plot (Figure 4(b)). The pyroxene monzonites display regular trends between Al_2O_3, K_2O Na_2O, Fe_2O_3, CaO, and SiO_2; however, there are no obvious correlations between the other major oxides and SiO_2 in the dioritic porphyrties (Figure 5).

The pyroxene monzonites and dioritic porphyrites were all characterized by light rare earth element (LREE) enrichment and heavy rare earth element (HREE) depletion, with a wide range La_N/Yb_N values (27–58) and moderate to small negative Eu anomalies ($Eu/Eu^* = 0.7–0.9$; Figure 6(a)). In the primitive mantle-normalized trace element diagrams, the pyroxene monzonites and dioritic porphyrites display an enrichment in large ion lithophile elements (i.e. Rb, Ba, Pb, and Th) and depletion in Sr and high field strength elements (i.e. Nb, Ta, P, and Ti; Figure 6(b)).

Sr–Nd–Pb isotopic ratios

Sr, Nd, and Pb isotopic data have been obtained from representative pyroxene monzonites and dioritic porphyrites (Table 3). The pyroxene monzonites and dioritic porphyrites exhibit very uniform ($^{87}Sr/^{86}Sr)_i$ and $\varepsilon_{Nd}(t)$ values, respectively. Such values include (as)

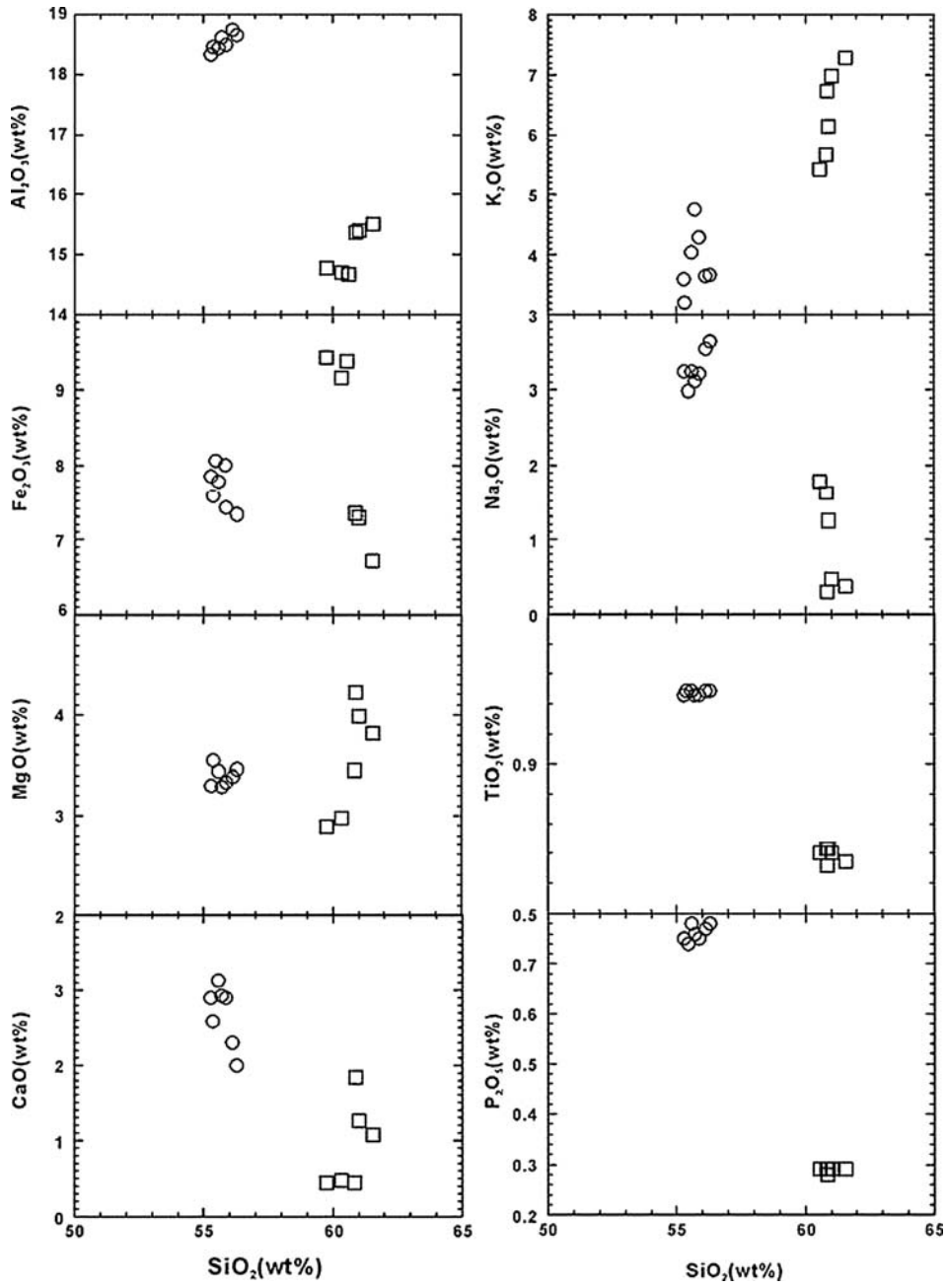

Figure 5. Selected variation diagrams of major element oxides versus SiO_2 plots for the pyroxene monzonites and dioritic porphyrites from the Sulu belt.

the $(^{87}Sr/^{86}Sr)_i$ ratios, which range from 0.709302 to 0.709303 for the pyroxene monzonites and from 0.708262 to 0.708267 for the dioritic porphyrites, while the $\varepsilon_{Nd}(t)$ values vary from -14.6 to -14.8 for the pyroxene monzonites and from -19.2 to -19.0 for the dioritic porphyrites. This suggests a different source region. In addition, the Sr–Nd isotopic compositions are comparable to those of the Neoproterozoic granites

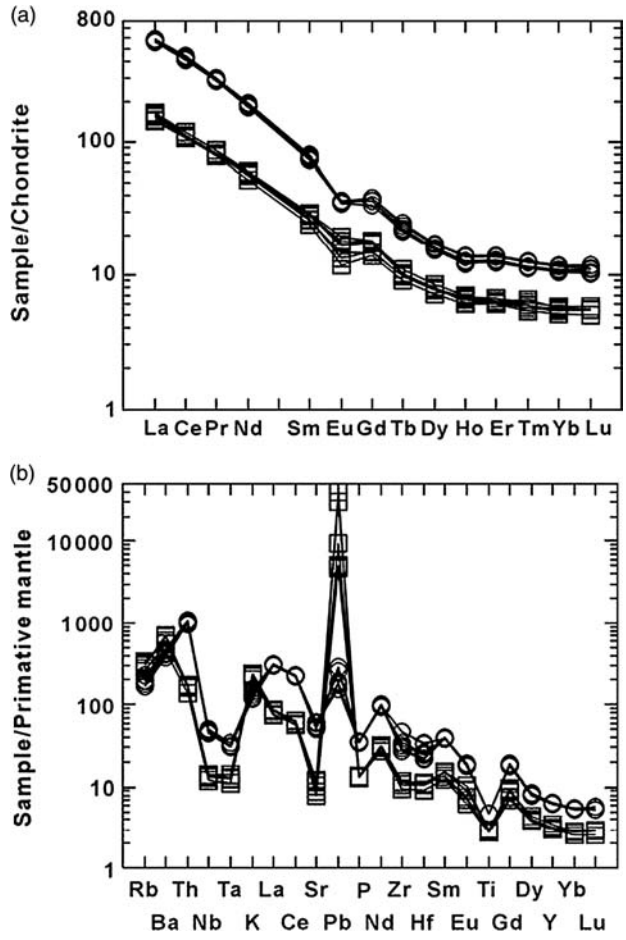

Figure 6. Chondrite-normalized rare earth element diagrams (a) and primitive mantle-normalized incompatible element distribution spidergrams (b) for the pyroxene monzonites and dioritic porphyrites from the Sulu belt. The normalization values are from Sun and McDonough (1989).

(recalculated to 120 Ma) and late Mesozoic magmatic rocks from the Sulu orogenic belt (Zhao *et al.* 1997; Zhou and Lu 2000; Fan *et al.* 2001; Guo *et al.* 2004, 2006; Huang *et al.* 2005; Meng *et al.* 2005; Yang *et al.* 2005a,b), but are inconsistent with those of the Neoproterozoic gabbros (recalculated to 120 Ma) in the Sulu belt (Figure 7).

The Pb isotopic ratios in the intrusive complexes are characterized by $^{206}Pb/^{204}Pb = 16.65–17.18$, $^{207}Pb/^{204}Pb = 15.33–15.54$, and $^{208}Pb/^{204}Pb = 36.83–38.29$. They are significantly different from those of the Yangtze lithospheric mantle (Yan *et al.* 2003), and are identical to those of the mafic rocks from Northern China Craton and Dabie orogen (Yan *et al.* 2003; Zhang *et al.* 2004; Xie *et al.* 2006), having a clear EM I affinity (Figure 8(a,b)).

Petrogenesis discussion

Source features

The intrusive complexes are characterized by moderate SiO_2 (55.28–61.57 wt%), suggesting that they could not have been derived from an intermediate-acid crust source, as partial

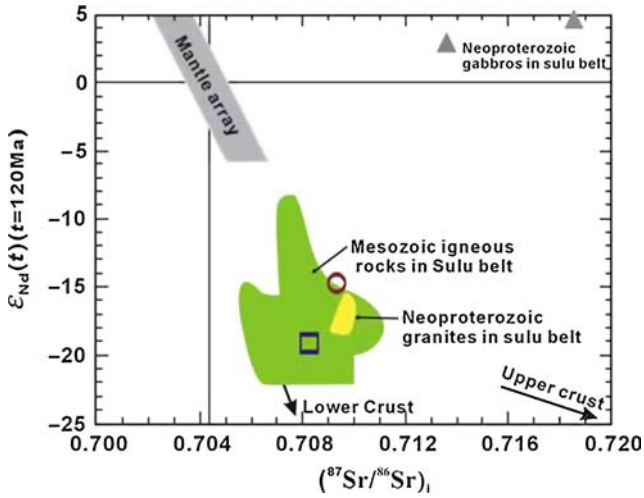

Figure 7. Initial $^{87}Sr/^{86}Sr$ versus $\varepsilon_{Nd}(t)$ diagram for the pyroxene monzonites and dioritic porphyrites from the Sulu belt. Other Mesozoic igneous rocks (Fan *et al.* 2001; Guo *et al.* 2004; Yang *et al.* 2005a,b; Huang *et al.* 2005; Meng *et al.* 2005; Guo *et al.* 2004; Guo *et al.* 2006; Zhao *et al.* 1997; Zhou and Lu 2000) and Neoproterozoic granites and gabbros (Huang *et al.* 2005) from the Sulu belt are also plotted.

melting of any of the exposed crustal rocks (e.g. Hirajima *et al.* 1990; Yang *et al.* 1993; Zhang *et al.* 1994; Kato *et al.* 1997) and lower crustal intermediate granulites (Gao *et al.* 1998a,b) in the deep crust would produce high-Si, low-Mg liquids (i.e. granitoid liquids; Rapp *et al.* 2003). Combining this with their high initial $^{87}Sr/^{86}Sr$ ratios and negative $\varepsilon_{Nd}(t)$ values (Table 3), we propose that the pyroxene monzonites and dioritic porphyrites may have resulted from a partial melting of the basaltic lower crust or enriched lithospheric mantle.

Experimental studies indicate that dehydration melting of the basaltic lower crust may have produced melts with intermediate compositions, especially in certain regions with high-heat flow values (Beard and Lofgren 1991; Rushmer 1991; Wolf and Wyllie 1994; Rapp and Watson 1995). The zircon oxygen isotopic compositions ($\delta^{18}O$) of the diorites from the Wulian region range from 5.07 to 6.43‰ (Huang *et al.* 2005), suggesting that the diorites could be produced by dehydration melting of the basaltic lower crust rather than the assimilation and contamination process of mantle-derived magma. The pyroxene monzonites share distinct chemical and isotopic compositions with dioritic porphyrites, favouring a different source. Accordingly, partial melting of the enriched lithospheric mantle is thought to be the most likely origin of the pyroxene monzonites discussed here. Nevertheless, the pyroxene monzonites are characterized by marked negative Nb anomalies and slightly positive Pb anomalies on the spidergram (Figure 6(b)), which is consistent with the involvement of crustal compositions (Rudnick and Fountain 1995). The pyroxene monzonites have high initial $^{87}Sr/^{86}Sr$ ratios (0.7093) and negative. $\varepsilon_{Nd}(t)$ values (−14.8 to − 14.6; Table 3; Figure 7), which, together with their high Zr/Hf (47–51) and Th/U (7.8–9.2) ratios (Table 2), indicate that the lower crust, but not the middle-upper crustal component, is involved in the generation of these rocks (Rudnick and Fountain 1995). Furthermore, the very uniform Sr and Nd isotopic compositions (Table 3; Figure 7) exclude significant crustal assimilation during magma ascent. Consequently, the involvement of the lower crustal materials occurred in the lithospheric mantle due to subduction or foundering. The widespread Mesozoic intermediate-acid rocks are

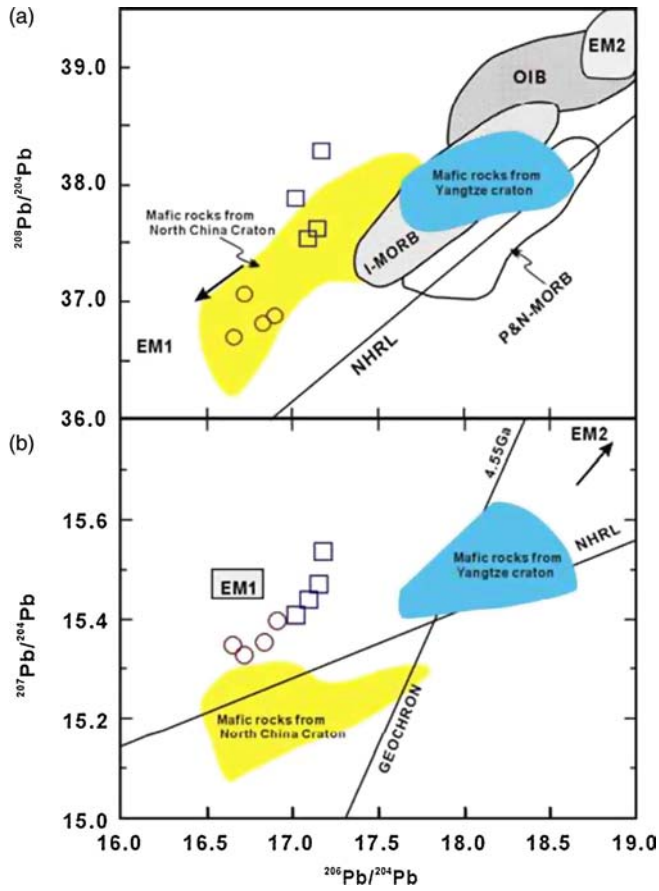

Figure 8. $^{208}Pb/^{204}Pb$ and $^{207}Pb/^{204}Pb$ versus $^{206}Pb/^{204}Pb$ diagrams for the pyroxene monzonites and dioritic porphyrites compared with those of the Early Cretaceous mafic rocks from the North China and Yangtze cratons. Fields for I-MORB (Indian MORB) and P&N-MORB (Pacific and North Atlantic MORB), OIB, NHRL and 4.55 Ga geochron are after Barry and Kent (1998), Zou *et al.* (2000), and Hart (1984), respectively. The data on north China craton are from Zhang *et al.* 2004 and Xie *et al.* (2006), the Yangtze mafic rocks are after Yan *et al.* (2003).

considered to be the result of a contribution of the subducted Yangtze Craton continental crust (Zheng *et al.* 2003; Zhao *et al.* 2004, 2005; Yang *et al.* 2005a,b). Based on this model, the pyroxene monzonites are expected to share similar Pb isotopic characteristics with the Yangtze lithosphere ($^{206}Pb/^{204}Pb = 17.649–18.603$, $^{207}Pb/^{204}Pb = 15.422–15.623$, $^{208}Pb/^{204}Pb = 7.674–38.521$; Chen *et al.* 2001; Yan *et al.* 2003; Xie *et al.* 2006). However, this is not the case (Figure 8(a,b)). Therefore, we argue that the pyroxene monzonites were formed by a recycling of the subducted Yangtze Craton continental crust. Overall, we consider the foundering of the lower crust to be a model for deciphering the involvement of crustal components in the source.

Fractional crystallization

The decreasing Fe_2O_3 and CaO during the course of magmatic evolution indicate separation of the ferromagnesian minerals (e.g. biotite, hornblende, clinopyroxene).

The pronounced depletions in Sr, Nb, Ta, P, Ti, and Eu (Figure 6(b)) demonstrate an advanced fractional crystallization during the formation of these complexes. Separation of the Ti-bearing phases (such as ilmenite and titanite) as well as apatite resulted in depletion in Nb (Ta)–Ti and P, respectively. Potent Sr and Eu depletion requires extensive fractionation of plagioclase and/or K-feldspar. It can be seen from the Sr versus Rb and Ba plots (Figure 9(a,b)) that there is a combined vector of plagioclase and K-feldspar fractionation for dioritic porphyrites; whereas there is plagioclase, K-feldspar, biotite, and hornblende fractionation for the pyroxene monzonites.

Zircon saturation thermometry (Watson and Harrison 1983) provides a simple and robust means of estimating intermediate-acid magma temperatures from bulk-rock compositions. The calculated zircon saturation temperatures (T_{Zr}) of the dioritic porphyrites were 812–823°C, whereas the T_{Zr} of the pyroxene monzonites ranged from 893 to 949°C. The distinct origin of the pyroxene monzonites is therefore also shown by their much higher values of zircon saturation temperatures (T_{Zr}) relative to the dioritic porphyrites.

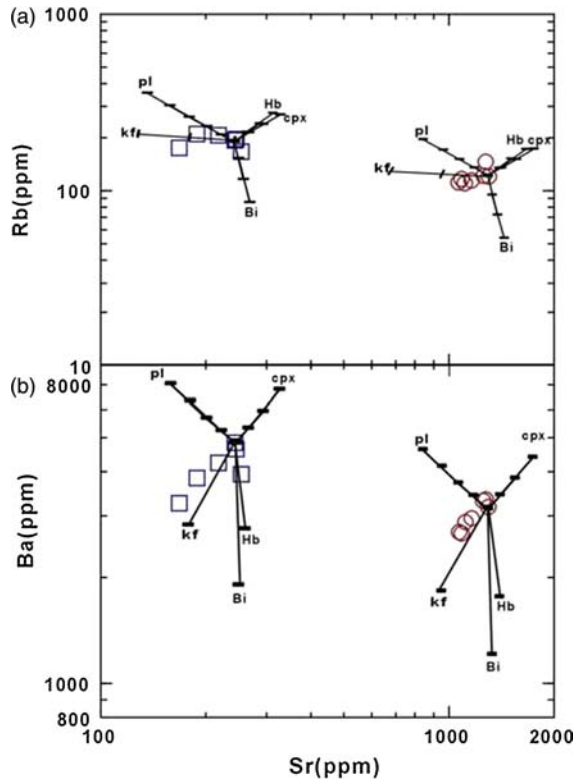

Figure 9. Plots of (a) Rb versus Sr and (b) Ba versus Sr for the pyroxene monzonites and dioritic porphyrites. Mineral fractionation vectors were calculated using the partition coefficients from Nash and Crecraft (1985) for biotite and K-feldspar, and Bacon and Druitt (1988) for hornblende and plagioclase, except for Mahood and Hildreth (1983) for the Ba in biotite and Arth (1976) for the Ba in K-feldspar. The tick marks indicate the percentage of mineral phase removed, in 10% intervals. cpx, clinopyroxene; pl, plagioclase; kf, potassium feldspar; Hb, hornblende, and Bi, biotite.

Genetic models

Mesozoic Diorites in the Wulian region were derived from a partial melting of the basaltic lower crust (Huang *et al.* 2005) induced by the activity of the plume during the Early Cretaceous (Zhao *et al.* 2004, 2005). However, there has been no direct evidence up to now suggesting the existence of Mesozoic plume activities in the Sulu belt. Therefore, we argue that the Mesozoic magmatism of the Sulu orogenic belt is related to the activity of the plume.

Alternatively, the late Mesozoic subduction of the palaeo-Pacific (Izanagi) plate (e.g. Chen *et al.* 2004) has been proposed to account for the petrogenesis of the Mesozoic magmatism of eastern China. The melts from the subducted Pacific plate metasomatized and modified the lithospheric mantle beneath eastern China (Chen *et al.* 2004). The subduction of the Pacific plate caused the extension of the continental lithosphere beneath eastern China (Tian *et al.* 1992). The lithosphere extension then induced decompression melting of the lithospheric mantle beneath eastern China, which produced the Mesozoic intense magmatism found in eastern China. Nevertheless, the late Mesozoic was a period when the Izanagi plate primarily moved toward the north or north-northeast (Maruyama and Send 1986; Kimura *et al.* 1990), thus affording little chance for inducing a broad back arc extension in this region. We thus rule out the effect of the subduction of the Pacific plate on the Mesozoic magmatic activities in the Sulu belt.

The foundering of the continental lower crust into the underlying convection mantle has been proposed to play a role in plume magmatism, crustal evolution and the formation of chemical heterogeneities within the mantle (Arndt and Goldstein 1989; Kay and Kay 1991; Rudnick and Fountain 1995; Jull and Kelemen 2001; Escrig *et al.* 2004; Gao *et al.* 2004, 2008; Elkins-Tanton 2005; Lustrino 2005; Anderson 2006). This is due to the unique chemical and physical properties of the eclogites formed by high to ultrahigh pressure metamorphism of basaltic rocks. Based on the above discussions, we prefer the more likely model advocated by Gao *et al.* (2008) to interpret the petrogenesis of the pyroxene monzonites. In this model, as the eclogites formed at the base of thickened continental crust, they had a higher density than lithospheric mantle peridotite by $0.2-0.4\,\mathrm{g\ cm^{-3}}$ (Rudnick and Fountain 1995; Jull and Kelemen 2001; Anderson 2006; Levander *et al.* 2006), and they sank into the subcrustal mantle (Arndt and Goldstein 1989; Kay and Kay 1991; Jull and Kelemen 2001; Gao *et al.* 2004). On the other hand, eclogites have a lower melting temperature than mantle peridotites (Yaxley and Green 1998; Rapp *et al.* 1999; Yaxley 2000; Kogiso *et al.* 2003; Sobolev *et al.* 2005, 2007), consequently, when the foundered silica-saturated eclogites were heated by the relatively hot subcrustal mantle coupled with the flux of heat from the upwelling asthenosphere, they produced silicic melts (tonalite to trondhjemite), which can variably hybridize with the overlying mantle peridotite. Such a reaction would produce an olivine-free pyroxenite, which, if subsequently melted, would in turn generate basaltic melts (Kogiso *et al.* 2003; Sobolev *et al.* 2005, 2007; Herzberg *et al.* 2006; Gao *et al.* 2008). Subsequently, the underplating of the basaltic magma would induce dehydration melting of the basaltic lower crust and the generation of dioritic magmas. Finally, basaltic magma fractionation took place, and this formed the pyroxene monzonites.

A scenario for the origin of the intrusive complexes in the Sulu belt is presented in Figure 10 based on the above model. Before 185 Ma, the collision between the North China Craton and Yangtze Craton resulted in a thickened crust (Figure 10(a)) and the peak metamorphism of HP–UHP terrane (Guo *et al.* 2006 and the references therein). During $185 \sim 165$ Ma, lithospheric delamination, mainly a foundering of eclogites from the lower thickened crust, occurred beneath the Dabie–Sulu orogenic belt (Li *et al.* 2002),

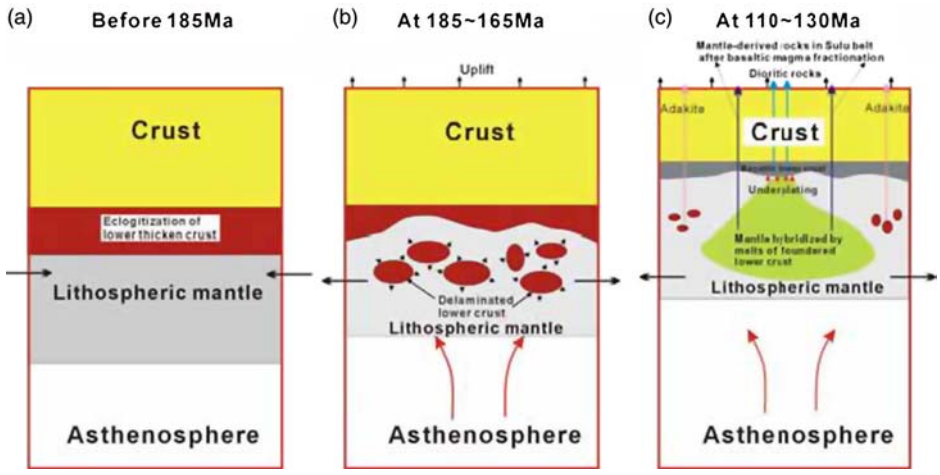

Figure 10. A schematic showing the lithospheric evolution and related magmatism beneath the Sulu belt. (a) Before 185 Ma, a thick crust formed due to subduction between the Yangtze Craton and north China Craton and induced eclogitization of the lower crust (Guo *et al.* 2006 and the references therein. (b) During 185–165 Ma, the higher density (relative to peridotite) eclogitized lower thickened crust foundered into the lithospheric mantle (Li *et al.* 2002), which triggered asthenospheric upwelling, orogenic collapse, and lithospheric extension beneath the Sulu belt, as well as a reaction between the mantle peridotite and the melts of the foundered lower crust. (c) Between 130 and 110 Ma, another lithospheric delamination occurred (mantle and lower crust) beneath the Dabie–Sulu orogenic belt (Li *et al.* 2002). Subsequently, decompressional melting of the hybridized lithospheric mantle produced primary magma (basaltic melts), with subsequent magma underplating and fractionation that occurred and formed the pyroxene monzonites and dioritic porphyrites identified in this study. In addition, the remaining eclogitic lower crusts in the lithospheric mantle were heated and produced the adakitic lavas of the Sulu belt (Guo *et al.* 2006; Liu *et al.* 2009).

which triggered asthenospheric upwelling, sudden uplift of the Sulu belt, orogenic collapse and lithospheric extension and thinning. Subsequently, silicic melts which were originated by the melting of the foundered eclogites reacted extensively with the subcrustal mantle peridotite (Figure 10(b)). Between 130 and 110 Ma, the second lithospheric delamination took place beneath the Dabie–Sulu orogenic belt (the mantle and lower crust; Li *et al.* 2002), while decompressional melting of the hybridized lithospheric mantle produced primary magma (basaltic melts). Subsequent underplating and fractionation of the basaltic melts induced the generation of the intrusive complexes in the Sulu belt (Figure 10(c)). In addition, the eclogitic lower crust remaining from the delamination event was heated in the lithospheric mantle and produced the adakitic lavas of the Sulu belt (Guo *et al.* 2006; Liu *et al.* 2009; Figure 10(c)). This model has been successfully applied to determine the origin of the mafic dikes in Luxi (Liu *et al.* 2008a,b).

Conclusions

Based on the geochronological, geochemical, and Sr–Nd–Pb isotopic studies, the following conclusions may be reached.

(1) The U–Pb zircon dating results indicate that the dioritic porphyrites were formed at 127.4 ± 1.2 Ma, together with the pyroxene monzonites (126 Ma); they are all the result of post-orogenic magmatism.

(2) The dioritic porphyrites and pyroxene monzonites resulted from different sources. The parental magma of the pyroxene monzonites was originated by the partial melting of an enriched lithospheric mantle hybridized by melts of foundered lower crust. Subsequent fractionation of clinopyroxene, K-feldspar, plagioclase, biotite, hornblende, ilmenite, or rutile resulted in the pyroxene monzonites with negligible crustal contamination. Alternatively, the primary magma of dioritic porphyrites were derived from partial melting of basaltic lower crust due to the underplating of basaltic magmas, and undertook plagioclase and K-feldspar fractionation without significant crustal contamination. The calculated zircon saturation temperatures (T_{Zr}) of the dioritic porphyrites were 812–823°C, whereas the T_{Zr} of the pyroxene monzonites range from 893 to 949°C. These approximately represent the crystallization temperature of the magmas.

(3) The inherited zircon age (757 ± 4.8 Ma ($n = 9$)) indicates that Neoproterozoic batholith is present beneath the Wulian region.

Acknowledgements

This research was supported by the Knowledge innovation project (KZCX2-YW-111-03) and the National Nature Science Foundation of China (40673029, 40773020, 90714010, 40634020). We are grateful to Gui-xiang Yu for helping to analyse Sr, Nd, and Pb isotopes. Dr Xiao-ming Liu, Hong-Lin Yuan and Shao-cong Lai are thanked for their help with Zircon U–Pb dating.

References

Anderson, D.A., 2006, Speculations on the nature and cause of mantle heterogeneity: Tectonophysics, v. 146, p. 7–22.

Arndt, N.T., and Goldstein, S.L., 1989, An open boundary between lower continental crust and mantle: Its role in crust formation and crustal recycling: Tectonophysics, v. 161, p. 201–212.

Arth, J.G., 1976, Behaviour of trace elements during magmatic processes: A summary of theoretical models and their applications: Journal of Research of the US Geological Survey, v. 4, p. 41–47.

Bacon, C.R., and Druitt, T.H., 1988, Compositional evolution of the zoned calcalkaline magma chamber of Mount Mazama Crater Lake, Oregon: Contributions to Mineralogy and Petrology, v. 98, p. 224–256.

Barry, T.L., and Kent, R.W., 1998, Cenozoic magmatism in Mongolia and the origin of central and east Asian basalts, *in* Flower, M.F.J., Chung, S.L., Lo, C.H., and Lee, T.Y., eds., Mantle Dynamics and Plate Interactions in East Asia. American Geophysical Union-Geodynamics Series, p. 347–364.

Beard, J.S., and Lofgren, G.E., 1991, Dehydration melting and water saturated melting of basaltic and andesitic greenstones and amphibolites at 1, 3, 6, 9 kb: Journal of Petrology, v. 32, p. 365–401.

Bureau of Geology and Mineral Resources of Shandong Province (BGMRS), 1991a, Regional geology of Shandong province. Beijing: Geological Publishing House, p. 594 (in Chinese).

Bureau of Geology and Mineral Resources of Shandong Province (BGMRS), 1991b, Attached map 2 of regional geology of Shandong province. Geological Publishing House, Beijing (in Chinese).

Chen, J.F., Yan, J., Xie, Z., Xu, X., and Xing, F.M., 2001, Nd and Sr isotopic compositions of igneous rocks from the Lower Yangtze region in eastern China: Constraints on sources: Physics and Chemistry of the Earth, Part A, v. 26, p. 719–731.

Chen, J.F., Xie, Z., Li, H.M., Zhang, X.D., Zhou, T.X., Park, Y.S., Ahn, K.S., Chen, D.G., and Zhang, H., 2003, U–Pb zircon ages for a collision-related K-rich complex at Shidao in the Sulu ultrahigh pressure terrane, China: Chemical Geology, v. 37, p. 35–46.

Chen, B., Jahn, B.M., Arakawa, A., and Zhai, M.G., 2004, Petrogenesis of the Mesozoic intrusive complexes from the southern Taihang Orogen, North China Craton and Sr–Nd–Pb isotopic constraints: Contributions to Mineralogy and Petrology, v. 148, p. 489–501.

Cheng, X., Cheng, J., and Wang, J., 1998, Element geochemistry of shoshonitic lamprophyres in the Pengjiakuang gold district, Shandong Province, China: Geochimica (in Chinese with English abstract) v. 27, p. 91–100.
Cong, B.L., ed., 1996, Ultrahigh-Pressure Metamorphic Rocks in the Dabie–Sulu Region of China. Beijing/Dordrecht: Science Press/Kluwer Academic Publishing, p. 224.
Elkins-Tanton, L.T., 2005, Continental magmatism caused by lithospheric delamination, *in* Foulger, G.R., Natland, J.H., Presnall, D.C., and Anderson, D.L., eds., Plates, plumes, and paradigms. Geological Society of America Special Paper 388, p. 449–462.
Escrig, S., Capmas, F., Dupré, B., and Allégre, C.J., 2004, Osmium isotopic constraints on the nature of the DUPAL anomaly from Indian mid-ocean-ridge basalts: Nature, v. 431, p. 59–63.
Fan, W.M., Guo, F., Wang, Y.J., Lin, G., and Zhang, M., 2001, Postorogenic bimodal volcanism along the Sulu orogenic belt in eastern China: Physics and Chemistry of the Earth A, v. 26, p. 733–746.
Gao, S., Luo, T.C., Zhang, B.R., Zhang, H.-F., Han, Y.W., Zhao, Z.D., and Hu, Y.K., 1998a, Chemical composition of the continental crust as revealed by studies in East China: Geochimica et Cosmochimica Acta, v. 62, p. 1959–1975.
Gao, S., Zhang, B.R., Jin, Z.M., Kern, H., Luo, T.C., and Zhao, Z.D., 1998b, How mafic is the lower continental crust? Earth and Planetary Science Letters, v. 106, p. 101–117.
Gao, S., Rudnick, R., Yuan, H.L., Liu, X.M., Liu, Y.S., Xu, W.L., Ling, W.L., Ayers, J., Wang, X.C., and Wang, Q.H., 2004, Recycling lower continental crust in the north China craton: Nature, v. 432, p. 892–897.
Gao, S., Rudnick, R.L., Xu, W.L., Yuan, H.L., Liu, Y.S., Walker, R.J., Puchtel, I., Liu, X.M., Huang, H., Wang, X.R., and Yang, J., 2008, Recycling deep cratonic lithosphere and generation of intraplate magmatism in the North China Craton: Earth and Planetary Science Letters, v. 270, p. 41–53.
Guo, F., Fan, W.M., Wang, Y.J., and Zhang, M., 2004, Origin of early Cretaceous calc-alkaline lamprophyres from the Sulu orogen in eastern China: Implications for enrichment processes beneath continental collisional belt: Lithos, v. 78, p. 291–305.
Guo, J.H., Chen, F.K., Zhang, X.M., Siebel, W., and Zhai, M.G., 2005, Evolution of syn-to post-collisional magmatism from north Sulu UHP belt,eastern China: Zircon U–Pb geochronology: Acta Petrologica Sinica, v. 21, p. 1281–1301.
Guo, F., Fan, W.M., and Li, C.W., 2006, Geochemistry of late Mesozoic adakites from the Sulu belt, eastern China: Magma genesis and implications for crustal recycling beneath continental collisional orogens: Geological Magazine, v. 143, p. 1–13.
Hart, S.R., 1984, A large-scale isotope anomaly in the southern Hemisphere mantle: Nature, v. 309, p. 753–757.
Herzberg, C., Asimow, P.D., Arndt, N., Niu, Y., Lesher, C.M., Fitton, J.G., Cheadle, M.J., and Saunders, A.D., 2006, Temperatures in ambient mantle and plumes: Constraints from basalts, picrites, and komatiites: Geochemistry Geophysics, Geosystems, v. 8, p. Q02006 doi:10.1029/2006GC001390.
Hirajima, T., Ishiwatari, A., Cong, B., Zhang, R., Banno, S., and Nozaka, T., 1990, Coesite from Mengzhong eclogite at Donghai county, northern Jiangsu province, China: Mineralogy Magazine, v. 54, p. 579–583.
Hong, D.W., Wang, T., Tong, Y., and Wang, X.X., 2003, Mesozoic granitoids from North China Block and Qinling–Dabie–Sulu orogenic belt and their deep dynamic process: Earth Science Frontiers, v. 10, p. 231–256.
Huang, J., Zheng, Y.F., Wu, Y.B., and Zhao, Z.F., 2005, Geochemistry of elements and isotopes in igneous rocks from the Wulian region in the Sulu orogen: Acta Petrologica Sinica, v. 21, p. 545–568.
Jahn, B.M., Cornichet, J., Cong, B.L., and Yui, T.F., 1996, Ultrahigh-ϵNd eclogites from an ultrahigh-pressure metamorphic terrane of China: Chemical Geology, v. 127, p. 61–79.
Jull, M., and Kelemen, P.B., 2001, On the conditions for lower crustal convective instability: Journal of Geophysical Research, v. 106, p. 6423–6446.
Kato, T., Enami, A., and Zhai, M., 1997, Ultrahigh-pressure marble and eclogite in the Su–Lu ultrahigh-pressure terrane, eastern China: Journal of Metamorphic Geology, v. 15, p. 169–182.
Kay, R.W., and Kay, S.M., 1991, Creation and destruction of lower continental crust: Geologische Rundschau, v. 80, p. 259–278.

Kimura, G., Takahashi, M., and Kono, M., 1990, Mesozoic collision extrusion tectonics in eastern Asia: Tectonophysics, v. 181, p. 15–23.
Kogiso, T., Hirschmann, M.M., and Frost, D.J., 2003, High-pressure partial melting of garnet pyroxenite: Possible mafic lithologies in the source of ocean island basalts: Earth and Planetary Science Letters, v. 216, p. 603–617.
Le Maitre, R.W., 2002, Igneous Rocks: A Classification and Glossary of Terms. 2nd ed. Cambridge: Cambridge University Press, p. 236.
Levander, A., Niu, F., Lee, C.T.A., and Cheng, X., 2006, Imaging the continental lithosphere: Tectonophysics, v. 416, p. 167–185.
Li, S.G., Jagoutz, E., Lo, C.H., Chen, Y.Z., and Li, Q.L., 1999, Sm/Nd, Rb/Sr and $^{40}Ar/^{39}Ar$ isotopic systematic of the ultrahigh-pressure metamorphic rocks in the Dabie–Sulu belt central China: A retrospective view: International Geology Review, v. 41, p. 1114–1124.
Li, S.G., Huang, F., and Li, H., 2002, Post-collisional delamination of the lithosphere beneath Dabie–Sulu orogenic belt: Chinese Science Bulletin, v. 46, p. 1487–1490.
Liu, S., Hu, R.Z., Gao, S., Feng, C.X., Qi, L., Zhong, H., Xiao, T.F., Qi, Y.Q., Wang, T., and Coulson, I.M., 2008a, Zircon U–Pb geochronology and major, trace elemental and Sr–Nd–Pb isotopic geochemistry of mafic dykes in western Shandong Province, east China: Constrains on their petrogenesis and dynamic significance: Chemical Geology, v. 255, p. 329–345 doi:10.1016/j.chemgeo.2008.07.006.
Liu, S., Hu, R.Z., Gao, S., Feng, C.X., Qi, Y.Q., Wang, T., Feng, G.Y., and Coulson, I.M., 2008b, U–Pb zircon age, geochemical and Sr–Nd–Pb–Hf isotopic constraints on age and origin of alkaline intrusions and associated mafic dikes from Sulu orogenic belt, Eastern China: Lithos, v. 106, p. 365–379.
Liu, S., Hu, R.Z., Gao, S., Feng, C.X., Yu, B.B., Qi, Y.Q., Wang, T., Feng, G.Y., 2009, Zircon U–Pb age, geochemistry and Sr–Nd–Pb isotopic compositions of adakitic volcanic rocks from Jiaodong, Shandong Province, Eastern China: constraints on petrogenesis and implications: Journal of Asian Earth Sciences, DOI:10.1016/jseaes.2009.02.008.
Lugmair, G.W., and Harti, K., 1978, Lunar initial $^{143}Nd/^{144}Nd$: Differential evolution of the lunar crust and mantle: Earth and Planetary Science Letters, v. 39, p. 349–357.
Lustrino, M., 2005, How the delamination and detachment of lower crust can influence basaltic magmatism: Earth-Science Reviews, v. 72, p. 21–38.
Mahood, G., and Hildreth, W., 1983, Large partition coefficients for trace elements in high silica rhyolites: Geochimica et Cosmochimica Acta, v. 47, p. 11–30.
Maruyama, S., and Send, T., 1986, Orogeny and relative plate motions: Example of the Japanese Islands: Tectonophysics, v. 127, p. 305–329.
Meng, F.C., Xue, H.M., Li, T.F., Yang, H.R., and Liu, F.L., 2005, Enriched characteristics of Late Mesozoic mantle under the Sulu orogenic belt: Geochemical evidence from gabbro in Rushan: Acta Petrologica Sinica, v. 21, p. 1583–1592.
Menzies, M., and Kyle, P.R., 1990, Continental volcanism: A crust-mantle probe, *in* Menzies, M.A., ed., Continental mantle. Oxford: Oxford University Press, p. 157–177.
Middlemost, E.A.K., 1972, A simple classification of volcanic rocks: Bulletin of Volcanology, v. 36, p. 382–397.
Middlemost, E.A.K., 1994, Naming materials in the magma/igneous rock system: Earth-Science Reviews, v. 74, p. 193–227.
Nash, W.P., and Crecraft, H.R., 1985, Partition coefficients for trace elements in silicic magmas: Geochimica et Cosmochimica Acta, v. 49, p. 2309–2322.
Potts, P.J., and Kane, J.S., 2005, International association of geoanalysts certificate of analysis: Certified reference material OU-6 (Penrhyn slate): Geostandards and Geoanlytical Research, v. 29, p. 233–236.
Qi, L., Hu, J., and Grégoire, D.C., 2000, Determination of trace elements in granites by inductively coupled plasma mass spectrometry: Talanta, v. 51, p. 507–513.
Rapp, R.P., and Watson, E.B., 1995, Dehydration melting of metabasalt at 8–32 kbar: Implications fro continental growth and crust–mantle recycling: Journal of Petrology, v. 36, p. 891–931.
Rapp, R.P., Shimizu, N., Norman, M.D., and Applegate, G.S., 1999, Reaction between slab-derived melts and peridotite in the mantle wedge: Experimental constraints at 3.8 GPa: Chemical Geology, v. 160, p. 335–356.
Rapp, R.P., Shimizu, N., and Norman, M.D., 2003, Growth of early continental crust by partial melting of eclogite: Nature, v. 425, p. 605–609.

Rudnick, R.L., and Fountain, D.M., 1995, Nature and composition of the continental crust: A lower crustal perspective: Reviews of Geophysics, v. 33, p. 267–309.
Rushmer, T., 1991, Partial melting of two amphibolites: Contrasting experimental results under fluid-absent conditions: Contributions to Mineralogy and Petrology, v. 107, p. 41–59.
Sobolev, A.V., Hofmann, A.W., Sobolev, S.V., and Nikogosian, I.K., 2005, An olivine-free mantle source of Hawaiian shield basalts: Nature, v. 434, p. 590–597.
Sobolev, A.V., Hofmann, A.W., Kuzmin, D.V., Yaxley, G.M., Arndt, N.T., Chung, S.-L., Danyushevsky, L.V., Elliott, T., Frey, F.A., Garcia, M.O., Gurenko, A.A., Kamenetsky, V.S., Kerr, A.C., Krivolutskaya, N.A., Matvienkov, V.V., Nikogosian, I.K., Rocholl, A., Sigurdsson, I.A., Sushchevskaya, N.M., and Teklay, M., 2007, The amount of recycled crust in sources of mantle-derived melts: Science, v. 316, p. 412–417.
Steiger, R.H., and Jäger, E., 1977, Subcommission on geochronology: Convention on the use of decay constants in geochronology and cosmochronology, Earth and Planetary Science Letters, v. 36, p. 359–362.
Sun, S.S., and McDonough, W.F., 1989, Chemical and isotopic systematics of oceanic basalts: Implications for mantle composition and processes, *in* Saunders, A.D., and Norry, M.J., eds., Magmatism in the Ocean Basins. London: Geological Society Special Publication, p. 313–345.
Thompson, M., Potts, P.J., Kane, J.S., and Wilson, S., 2000, An International Proficiency Test for Analytical Geochemistry Laboratories-Report on Round 5 (August 1999): Geostandards and Geoanlytical Research, v. 24, p. E1–E28.
Tian, Z.Y., Han, P., and Xu, K.D., 1992, The Mesozoic–Cenozoic East China rift system: Tectonophysics, v. 208, p. 341–363.
Wang, Y.M., Gao, Y.S., Han, H.M., and Wang, X.H., 2003, Practical handbook of reference materials for geoanalysis: Geological Publishing House (in Chinese).
Watson, E.B., and Harrison, T.M., 1983, Zircon saturation revisited: temperature and composition effects in a variety of crustal magma types: Earth and planetary Science Letters, v. 64, p. 295–304.
Wolf, M.B., and Wyllie, P.J., 1994, Dehydration melting of amphibolite at 10 kbar: Effects of temperature and time: Contributions to Mineralogy and Petrology, v. 115, p. 369–383.
Wu, Y.B., Zheng, Y.F., and Zhou, J.B., 2004, Neoproterozoic granitoid in northwest Sulu and its bearing on the North China–South China Blocks boundary in East China: Geophysical Research Letters, v. 31, p. Lo7616 doi:10.1029/2004GL019785.
Xie, Z., Li, Q.Z., and Gao, T.S., 2006, Comment on 'Petrogenesis of post-orogenic syenites in the Sulu orogenic belt, east China: Geochronological, geochemical and Nd–Sr isotopic evidence' by Yang *et al*., Chemical Geology, v. 235, p. 191–194.
Xu, J.W., and Zhu, G., 1994, Tectonic models of the Tan-Lu fault zone, eastern China: International Geology Review, v. 36, p. 771–784.
Yan, J., Chen, J.F., Yu, G., Qian, H., and Zhou, T.X., 2003, Pb isotopic characteristics of Late Mesozoic mafic rocks from the Lower Yangtze Region: Evidence for enriched mantle: Journal of China University of Geosciences, v. 9, p. 195–206 (in Chinese).
Yang, J., Godard, G., Kienast, J.R., Lu, Y., and Sun, J., 1993, Ultrahighpressure 60 kbar magnesite-bearing garnet peridotites from northeastern Jiangsu, China: Journal of Geology, v. 101, p. 541–554.
Yang, J.H., Chung, S.L., Wilde, S.A., Wu, F.Y., Chu, M.F., Lo, C.H., and Fan, H.R., 2005a, Petrogenesis of post-orogenic syenites in the Sulu Orogenic Belt, East China: Geochronological, geochemical and Nd–Sr isotopic evidence: Chemical Geology, v. 214, p. 99–125.
Yang, J.H., Wu, F.Y., Chung, S.L., Wilde, S.A., Chu, M.F., Lo, C.H., and Song, B., 2005b, Petrogenesis of Early Cretaceous intrusions in the Sulu ultrahigh-pressure orogenic belt: East China and their relationship to lithospheric thinning: Chemical Geology, v. 222, p. 200–231.
Yang, J.H., and Zhou, X.H., 2001, Rb-Sr, Sm-Nd, and Pb isotope systematics of pyrite: implications for the age and genesis of lode deposits: Geology, v. 29, p. 711–714.
Yaxley, G.M., 2000, Experimental study of the phase and melting relations of homogeneous basalt plus peridotite mixtures and implications for the petrogenesis of flood basalts: Contributions to Mineralogy and Petrology, v. 139, p. 326–338.
Yaxley, G.M., and Green, D.H., 1998, Reactions between eclogite and peridotite: Mantle refertilisation by subduction of oceanic crust: Schweizer Mineralogische and Petrographische Mitteilungen, v. 78, p. 243–255.

Ye, K., Hirajima, T., and Ishiwateri, A., 1996, Significance of interstitial coesite in eclogites from Yankou, Qingdao city, eastern China: Chinese Science Bulletin, (in Chinese) v. 41, p. 1047–1048.

Ye, K., Ye, D.N., and Cong, B.L., 2000, The possible subduction of continental material to depths greater than 200 km: Nature, v. 407, p. 734–736.

Yin, A., and Ni, S., 1993, An indentation model for the north and south China collision and the development of the Tan-Lu and Honam fault systems, eastern Asia: Tectonics, v. 124, p. 801–813.

Yuan, H.L., Gao, S., Liu, X.M., Li, H.M., Gunther, D., and Wu, F.Y., 2004, Accurate U–Pb age and trace element determinations of zircon by laser ablation–inductively coupled plasma mass spectrometry: Geostandard Newsletters, v. 28, p. 353–370.

Zhang, R.Y., Liou, J.G., and Cong, B., 1994, Petrogenesis of garnetbearing ultramafic rocks and associated eclogites in the SuLu ultrahigh–P metamorphic terrane, eastern China: Journal of Metamorphic Geology, v. 12, p. 169–186.

Zhang, H.F., Sun, M., Zhou, M.F., Fan, W.M., Zhou, X.H., and Zhai, M.G., 2004, Highly heterogeneous Late Mesozoic lithospheric mantle beneath the North China Craton: Evidence from Sr–Nd–Pb isotopic systematics of mafic igneous rocks: Geological Magazine, v. 141, p. 55–62.

Zhao, G., Wang, D., and Cao, Q., 1997, Geochemical features and petrogenesis of Laoshan Granite in east Shandong Province: Geological Journal of China Universities (in Chinese with English abstract) v. 3, p. 1–15.

Zhao, Z.F., Zheng, Y.F., Wei, C.S., and Wu, Y.B., 2004, Zircon isotope evidence for recycling of subducted continental crust in post-collisional granitoids from the Dabie terrane in China: Geophysical Research Letters, v. 31, p. L22602, doi:10.1029/2004GL021061.

Zhao, Z.F., Zheng, Y.F., Wei, C.S., Wu, Y.B., Chen, F.K., and Jahn, B.M., 2005, Zircon U–Pb age, element and C–O isotope geochemistry of post-collisional mafic–ultramafic rocks from the Dabie orogen in east-central China: Lithos, v. 83, p. 1–28.

Zheng, Y.F., Wang, Z.R., Li, S.G., and Zhao, Z.F., 2002, Oxygen isotope equilibrium between eclogite minerals and its constraints on mineral Sm–Nd chronometer: Geochimica et Cosmochimica Acta, v. 66, p. 625–634.

Zheng, Y.F., Fu, B., Gong, B., and Li, H., 2003, Stable isotope geochemistry of ultrahigh pressure metamorphic rocks from the Dabie–Sulu orogen in China: Implications for geodynamics and fluid regime: Earth-Science Reviews, v. 62, p. 105–161.

Zhou, J.B., Zheng, Y.F., and Zhao, Z.F., 2003a, Zircon U–Pb Dating on Mesozoic Granitoids at Wulian, Shandong Province: Geological Journal of China Universities (in Chinese with English abstract) v. 9, p. 185–194.

Zhou, J.B., Zheng, Y.F., and Wu, Y.B., 2003b, Zircon U–Pb ages for Wulian granites in northwest Sulu and their tectonic implications: Chinese Science Bulletin, v. 48, p. 379–384.

Zhou, T.H., and Lu, G.X., 2000, Tectonics, granitoids and Mesozoic gold deposits in East Shandong, China: Ore Geology Reviews, v. 16, p. 71–90.

Zou, H.B., Zindler, A., Xu, X.S., and Qi, Q., 2000, Major, trace element, and Nd, Sr and Pb isotope studies of Cenozoic basalts in SE China: Mantle sources, regional variations and tectonic significance: Chemical Geology, v. 171, p. 33–47.